Detection of Patient's Bed Statuses in 3D Using A Microsoft Kinect

Yun Li, Lyle Berkowitz, Gary Noskin, Sanjay Mehrotra

Abstract— **Patients spend the vast majority of their hospital stay in an unmonitored bed where various mobility factors can impact patient safety and quality. Specifically, bed positioning and a patient's related mobility in that bed can have a profound impact on risks such as pneumonias, blood clots, bed ulcers and falls. This issue has been exacerbated as the nurse-per-bed (NPB) ratio has decreased in recent years. To help assess these risks, it is critical to monitor a hospital bed's positional status (BPS). Two bed positional statuses, bed height (BH) and bed chair angle (BCA), are of critical interests for bed monitoring. In this paper, we develop a bed positional status detection system using a single Microsoft Kinect. Experimental results show that we are able to achieve 94.5% and 93.0% overall accuracy of the estimated BCA and BH in a simulated patient's room environment.**

I. Introduction

Hospital quality and patient safety issues have been of increasing concern in the past few decades [1]. We propose that a critical, but often overlooked, component of patient quality and safety is related to a patient's in-bed behavior (IBB), where they often spend much of their hospital stay. Important IBBs include limb mobility, sleeping postures, wandering movement, head of bed positioning and bed entries and exits. For example, it has been shown that most falls occur in the patient's room during attempts to get in or out of bed [2]. These falls cause serious health problems such as trauma, fracture and even deaths [3]. Patient safety issues as such these can be addressed by sufficient monitoring and care delivery [1]. However, most hospitals rely on manual monitoring, which degrades nursing efficiency while still not ensuring a consistent outcome. In the past years, a few intelligent systems have been developed to monitor some specific IBBs, such as a commercial bed-exit alarm systems [4] and a proposed bed monitoring system using multi-modal sensors [5]. Although these systems have achieved promising performance, they still have many limitations. The bed-exit alarm systems are very costly and usually need to be reinitialized when the patient reenters the bed and reinstalled when the bed changes the position. The multi-modal sensors are costly, inconvenient to deploy and also intrusive for the patients.

Y. L. and S. M. are with Department of Industrial Engineering and Management Science, Northwestern University, Evanston, IL 60208, USA. (e-mail: yun.li@northwestern.edu, and corresponding author's e-mail: mehrotra@northwestern.edu)

L. B. and G. N. are with Feinberg School of Medicine, Northwestern University, Chicago, IL 60622, USA. (e-mail: lberkowi@nmh.org and gnoskin@nmh.org)

An IBB monitoring system using a single video camera is thus believed to provide a cheaper and easier alternative to detect abnormal behavior and prevent safety issues such as bed falls. A first step towards this type of system is a vision-based sensing device which provides good estimation of bed position or edges to reduce false alarms. The latest research work [6] has provided an effective approach to estimate the bed edges from color images. It also robustly measures slight changes of bed position, which is needed in the real world on of a patient's hospital room. However, this approach has three limitations which need to be addressed. First, a system which depends only on the color image information will fail in the dark. Second, a system which only estimates the bed edges in 2D will not be as effective as a 3D analysis. Third, there may be privacy issue related to the processing of color images. Our proposed system is able to monitor the patient's bed in various lighting changes and does not process any color information. In addition, it is able to provide 3D bed edges as well as bed statuses such as bed chair angle (BCA) and bed height (BH). Since patient beds with auto controls of BCA and BH are widely used in the patient's rooms, these measurements are important.

The Microsoft Kinect device [7] has motivated innovative solutions to the development of human-machine interactive applications based on its inexpensive price and effective depth sensor. The depth sensor provides the third dimension needed so that objects are able to be described in 3D patterns. Moreover, depth sensing is independent of visible lighting so that the system performs effectively in both light and dark environment. The Kinect has been recently utilized in healthcare applications such as the fall detection [8] and gait analysis [9].

In this paper, we utilize the Kinect depth information to estimate the 3D bed edges, BCA and BH. We have implemented the proposed system in real time using Kinect SDK [7] and openCV. The Kinect device was installed in a simulated patient room and bed statuses were monitored constantly through the graphic user interface (GUI) at the remote site. The experiments described were designed to evaluate the robustness of the system by introducing scenarios of lighting changes and slight bed position changes.

The rest of the paper is structured as follows: Section II describes the bed status detection algorithm using depth sensing. Section III presents experimental design, results and analysis. Section IV concludes the paper.

II. Bed Statuses Detection using Depth Sensing

A. General description of Kinect depth sensing

Kinect depth image is generated by the laser light patterns. The pixel intensity of the depth image is in

978-1-4244-7929-0/14/$26.00 ©2014 IEEE

grayscale and is proportional to the physical distance between the nearest object at that pixel location and the sensor center. Therefore Kinect is able to estimate the 3D pattern of the objects in its skeleton coordinate system. The depth resolution is 480 × 640 pixels and the operating range is around 2 ~ 5 meters. Objects out of the range will produce invalid pixels of zero intensity. Interesting readers please refer to [7].

B. *The proposed 4-phase bed statuses detection algorithm*

Figure 1 depicts the proposed 4-phase bed statuses detection algorithm using depth sensing. Figure 1-(a) shows a frame of raw color image in which the patient's bed (Hill-Rom Advance2000) is placed in the center of the room. The bed consists of two sections. The surface in pink is called head section which rises at certain BCA; the other in light green is called foot section which is placed horizontally but elevates at certain BH. Each phase is specifically described in the following context.

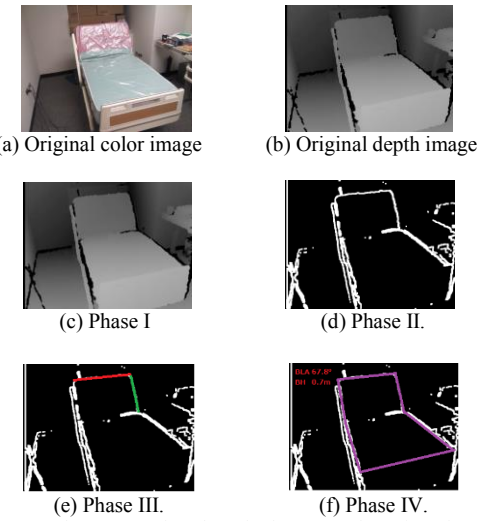

(a) Original color image (b) Original depth image

(c) Phase I (d) Phase II.

(e) Phase III. (f) Phase IV.

Figure 1. The proposed 4-phase bed statuses detection algorithm using Kinect depth sensing.

1) *Phase I. Frames average*

The corresponding depth image is shown in Figure 1-(b). In real-time applications, depth frames are sequentially captured and processed. We have observed that over sequential raw depth frames the area around the bed edges usually produces flickering effects, making the edge shape highly noisy and unstable. The noisy edges will result to poor edges and lines detection in the following phases. Gaussian blur [10] and moving average are the most effective refinement filters to reduce edge noise. To reduce the computational cost, we utilize a simple exponential weighted moving average as described by

$$U'_t = \alpha U_t + (1-\alpha)U'_{t-1} \quad (t = 1,2,\dots) \qquad (1)$$

where U_t represents the current captured raw depth frame at time t; U'_t and U'_{t-1} represent the averaged frame at time t and $t-1$. U'_t is used for processing and updating U'_{t-1}. U'_0 is initialized as all zeros. In the preliminary experiments, we found that the forgetting factor $\alpha = 0.4$ is sufficient to reduce the edge noise and make the edges more stable in sequential processing frames (see Figure 1-(c)). This will improve the performance in the following phases. Smaller α (α <0.3) will dramatically degrade the real-time performance since it takes more time to adapt to changing bed statuses.

2) *Phase II. Edge detection and dilation*

Edge detection followed by the dilation process is then applied to U'_t. We use the traditional Sobel edge detector provided by openCV. The output grayscale image with detected edges is then converted to a binary image. To further reduce the residual noise on the edges, dilation is then applied to the binary image with a kernel dimension of 3 by 3 pixels. Figure 1-(d) shows one frame of the processed binary image in which bed edges are detected.

3) *Phase III. Lines detection and classification*

Figure 2 shows the Kinect 2D depth image coordinate in which two lines are defined by their polar coordinate.

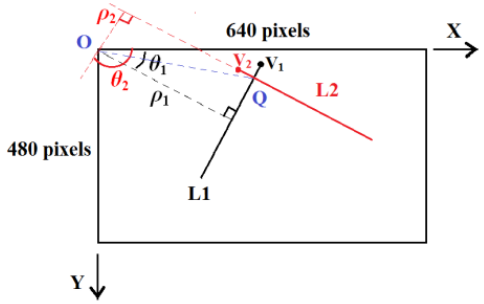

Figure 2. The polar coordinate representations (θ - ρ) of two solid lines L1 (θ_1, ρ_1) and L2 (θ_2, ρ_2) intersecting at point **Q** in the Kinect depth image coordinate (X - Y) with the resolution of 480 (Y) × 640 (X) pixels. $\mathbf{V_1}$ and $\mathbf{V_2}$ are the endpoints of L1 and L2 with the closest distance.

In Figure 2, two lines (L1 and L2) intersect at point Q are drawn in the image coordinate and their corresponding polar coordinate representations are defined as well with $\theta \in [0, 180^\circ)$ and $\rho \in \left(-640, \sqrt{640^2 + 480^2} = 800\right)$ in pixels. Note if L1 is perpendicular to L2, we have two constraints

$$|\theta_2 - \theta_1| = 90^\circ \text{ and} \qquad (2)$$

$$\rho_1^2 + \rho_2^2 = \|\boldsymbol{O} - \boldsymbol{Q}\|^2 . \qquad (3)$$

$\|\cdot\|$ denotes Euclidean norm of $\cdot$. The Hough transform presents that any line in the image domain has unique transform in the $\theta - \rho$ domain. Straight lines are then detected using Standard Hough Line Transform (SHLT) [11]. Without classification, the SHLT detects all the possible lines including the false positives not the part of the bed edges or outside the bed region. Therefore the following two assumptions are made for developing more robust lines classification algorithm.

Assumption 1. we assume that only the head line (HL) and head side line (HSL) of the head section as shown in red and green respectively in Figure 1-(e) are used for detection. The reason is that in a real patient's room, the patient usually has a blanket which covers most part of the foot section side edges and makes the edges highly noisy and unstable in the depth image. On the other hand, HL and HSL are rarely covered by any objects so they become the only but the most reliable features for bed statuses detection.

Assumption 2. we assume that the bed position changes in a slight transition among the three placement in Figure 3. The reason for this assumption is that in the real patient's room, the patient's bed is usually not placed at its original position

at each time after the patient receives the bedside caring or been ambulated from other departments.

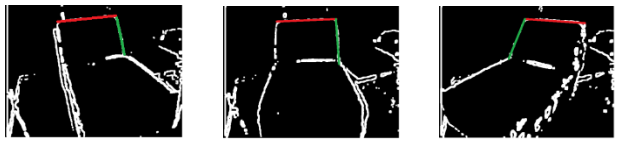

(a) (b) (c)

Figure 3. The common bed placement in a patient's room. (a) Rotate left; (b) Rotate left but almost right against the depth sensor; (c) Rotate right.

```
Δ For each depth frame:
    Do SHLT lines detection;
    For each detected line:
        Calculate θ and ρ;
        If 30 < ρ < 100
            If 70° < θ < 90°
                A HL is detected (the red line shown in Figure 3-(a) and (b));
                Choose Q as the right endpoint V of the detected HL;
                Set bed placement as 'Rotate left';
            Else if 90° ≤ θ < 110°
                A HL is detected (the red line shown in Figure 3-(c));
                Choose Q as the left endpoint V of the detected HL;
                Set bed placement as 'Rotate right';
            Else goto Δ;
        Else goto Δ;
    End for
    For each detected line:
        If bed placement is 'Rotate left'
            Calculate ρ⊥ of the line perpendicular to the detected HL using equation (3);
            Determine the endpoint V⊥ of the current line which is closest to Q;
            If 160° − α < θ < 180° and ρ⊥ − β < ρ < ρ⊥ + β and ||V − V⊥|| < δ
                A HSL is detected (the green line shown in Figure 3-(a) and (b));
        Else if bed placement is 'Rotate right'
            Calculate ρ⊥ of the line perpendicular to the detected HL using equation (3);
            Determine the endpoint V⊥ of the current line which is closest to Q;
            If 0 ≤ θ < 20° + α and ρ⊥ − β < ρ < ρ⊥ + β and ||V − V⊥|| < δ
                A HSL is detected (the green line shown in Figure 3-(c));
        Else goto Δ;
    End for
End for
```

Figure 4. The pseudo code for the lines classification algorithm.

Figure 4 shows the lines classification algorithm based on Assumption 1 and 2. Although physically HL and HSL are exactly perpendicular to each other, this is not true when they are displayed in the image. Thus we introduce factors α and β to relax the constraints of θ and ρ respectively so that the classification is more robust to the angle distortions in the image space. We choose α=20° and β=30 pixels for our settings. In addition, we choose $\delta = 20$ pixels to filter out the lines which do not intersect or are not close enough to the detected HL. In summary, the algorithm classifies HL first and determine the type of placement (rotate left or right), then classifies HSL based on the placement.

4) Phase IV. Bed statuses estimation on 3D point cloud

In this phase, the detected HL and HSL are used to generate the 3D bed edges, estimate BCA and BH. To achieve this purpose, N pixels with equal interval of $L/(N\text{-}1)$ (L is the line length) on the detected HL and HSL are chosen to be mapped into corresponding N-point cloud. The Kinect SDK provides the functionality to perform the mapping from depth image space to skeleton space and also estimate the ground plane equation [7]. The point clouds of the HL and HSL are used to generate their 3D regression lines using N-point ordinary least squares based regression. Once we have the 3D representations of HL and HSL, and if the length of the side edge of the foot section is also known, we are able to estimate all bed edges in 3D as shown in purple lines in Figure 1-(f).

To estimate BCA and BH, we suppose the Kinect SDK estimates the ground plane by

$$y = \hat{A}x + \hat{B}y + \hat{C}z + \hat{D}\,, \tag{4}$$

with its estimated normal vector $\hat{\boldsymbol{n}} = \left[\hat{A}, \hat{B}, \hat{C}\right]^T$. And the coordinate of the i^{th} point of the N-point cloud mapped from the detected HL is $\boldsymbol{p}_{\text{HL}}^i = [x_i, y_i, z_i]^T$, $i = 0,1,..,N-1$. Thus the distance between $\boldsymbol{p}_{\text{HL}}^i$ and the ground plane denoted by $\hat{h}_i$ is computed by

$$\hat{h}_i = \left|\hat{\boldsymbol{n}}^T \boldsymbol{p}_{\text{HL}}^i + \hat{D}\right| / \|\hat{\boldsymbol{n}}\|\,, \tag{5}$$

Then we take the average $\hat{h} = \frac{1}{N}\sum_{i=0}^{N-1} \hat{h}_i$. The regression model of HSL provides the estimation of both the length $\hat{l}$ and the unit vector $\boldsymbol{u}_{\text{HSL}}$ of the regressive line. Thus the estimated $\widehat{\text{BCA}}$, the angle between the regressive line and the ground plane is computed by

$$\widehat{\text{BCA}} = arcsin(|\hat{\boldsymbol{n}}^T \boldsymbol{u}_{\text{HSL}}| / \|\hat{\boldsymbol{n}}\|) \tag{6}$$

Figure 5 describes the bed configuration in the Kinect skeleton space. Therefore the estimated $\widehat{\text{BH}}$ is obtained by

$$\widehat{\text{BH}} = \hat{h} - \hat{l}\sin(\widehat{\text{BCA}})\,. \tag{7}$$

To reduce the high computational cost caused by N, we choose N=10 in this phase. In real environment, $\hat{l}$ is difficult to estimate since the HSL is usually blocked partially in the image by the patient's arms or the blanket. To improve the estimation accuracy of $\widehat{\text{BH}}$, we assume that $\hat{l}$ is known in advance (l = 0.6 meters for this particular bed model).

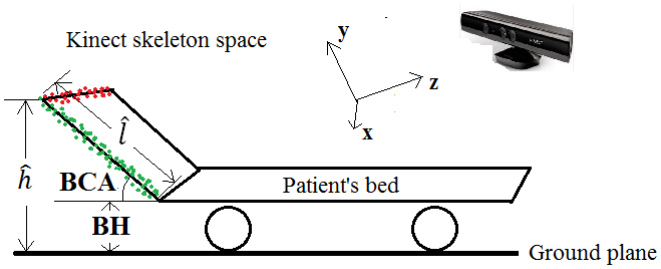

Figure 5. The configurations of the patient's bed in the Kinect skeleton space coordinate. Red dots represent the point cloud mapped from the detected HL and green dots represent the one mapped from the detected HSL.

III. Experimental Design, Results and Analysis

A. Experimental design

In the experiments, we are able to evaluate the accuracy of the BCA and BH estimated by the proposed system since we can read their groundtruths directly from the 'Head Angle and Elevation Indicator' located beneath the foot section of the bed. To evaluate the system, we collected two groups of data which consists of 4000 bed images taken in our simulated patient's room. Group I consists of 2000 images taken with the light on and Group II consists of the rest images taken with the light off (completely dark). For each group, 250 images were taken for one of the 8 scenarios as shown in Figure 6. In each scenario, the bed is placed at a different position with changing BCAs and BHs. We consider 5 BCAs — 0°, 15°, 30°, 45°, 60° (full raise) and 5

BHs in meters ─ 0.2, 0.4, 0.6, 0.8, 1.0. In each scenario, we have 10 images for each combination of BCA and BH.

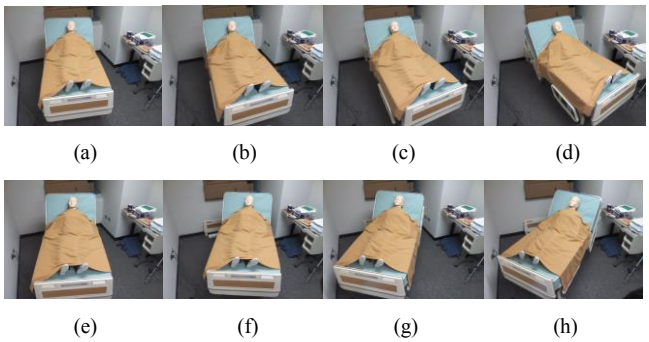

(a) (b) (c) (d)

(e) (f) (g) (h)

Figure 6. Images (a) – (h) show 8 scenarios of different bed positions. A human dummy is lying in the bed covered by a blanket to simulate the patient's room environment.

B. Experimental results and analysis

The performance is evaluated by calculating the root mean squared errors (RMSEs) of the estimated BCAs and BHs and the corresponding overall accuracy in percentage denoted by ACC (ACC=1 − RMSE / maximum operating ranges of BCA or BH). The results of each group are shown in Table I.

Table I. RMSEs and ACCs of the estimated BCAs in degrees and BHs in meters for Group I and Group II.

	Group I	Group II
BCA	RMSE 3.16º, ACC 94.7%	RMSE 3.34º, ACC 94.4%
BH	RMSE 0.07, ACC 93.0%	RMSE 0.07, ACC 93.0%

Table I shows that we are able to achieve about 94.5% and 93.0% overall estimation accuracy of BCA and BH respectively for both groups. The results also show that the detection performance in the lighting room (Group I) and dark room (Group II) makes no significant difference. This observation validates that the depth sensing is independent of visible light.

In the following, we provide the analysis of three possible reasons which cause the estimation errors and their solutions. 1) The poor estimation of the ground plane provided by Kinect SDK directly results to poor estimated BCAs and BHs according to equations (5-6). This device-related error can be reduced by calibrating the Kinect camera and using the calibrated intrinsic/extrinsic camera parameters to measure the ground plane in advance. 2) The small z-axis distance of the skeleton coordinate (Figure 5) between the background objects and the head section of the bed results to poor or no detection of HL and HSL edges due to the limited resolution of the depth intensity. In the preliminary experiments, we found that the distance larger than 0.3 meters is robust enough to detect the required edges. 3) The possible extension of the HL or HSL due to their alignment with false detected edges out of the bed region. This can be addressed by placing the bed against the background objects with smooth physical surface such as a wall. 2) and 3) are seen as the limitations of the proposed system but the restrictions for its real deployment are easily accommodated by most of the normal patient's rooms.

IV. CONCLUSIONS

This paper introduces a method to automatically detect a hospital bed's edges and statuses using depth sensing of a Kinect device. We were able to achieve 94.5% and 93.0% overall accuracy of the estimated BCA and BH in the simulated patient's room environment. The performance, although not sufficiently high for measurement purpose, is very promising for supporting patient safety projects.

This work establishes the base for the future development of various hospital in-bed applications such as bed-exit movement, bed-fall-prevent alarm and in-bed movement detection systems using Kinect depth sensing. In the next step, we will extend the current work by utilizing more robust computer vision techniques to improve the bed statuses estimation accuracy in more realistic environment, such as when the patient sits on the bed edges or doctors block the camera view. We will additionally generate an entire 3D model of the patient's bed using real hospital dataset.

The final result of this work will be to improve quality and safety in a hospital room. Examples may include the ability to alert a nurse if a patient's head of their bed is set incorrectly, if they have not moved in a certain period of time, or if they appear to be at high risk of falling.

REFERENCES

[1] A. Gruneir and V. Mor, "Nursing home safety: current issues and barriers to improvement," *Annu Rev Public Health*, vol. 29, pp. 369–382, 2008.

[2] E. B. Hitcho, M. J. Krauss, S. Birge, *et al*., "Characteristics and circumstances of falls in a hospital setting," *J Gen Intern Med*, vol. 19, pp. 732–739, 2004.

[3] D. A. Sterling, J. A. O'Connor and J. Bonadies, "Geriatric falls: injury severity is high and disproportionate to mechanism," *J Trauma–Injury, Infection and Critical Care*, vol. 50(1), pp. 116–119, 2001.

[4] E. Capezuti, B. L. Brush, **S.** Lane, H. U. Rabinowitz, and M. Secic, "Bed-exit alarm effectiveness," *Arch Gerontol Geriatr*, vol. 49, pp. 27–31, 2009.

[5] P. W. A. Aung, F. Foo, H. Weimin, B. Jit, J. Phua, L. Koujuch, and H. Chi-Chun, "Evaluation and analysis of multimodal sensors for developing in and around the bed patient monitoring system," in *Proc. 32th Int. IEEE EMBS Conf.,* Argentina, August, 2010, pp. 2159–2162.

[6] P. Kittipanya-Ngam, O. S. Guat, and E. H, Lung, "Bed Detection For Monitoring System In Hospital Wards," in *Proc. 34th Int. IEEE EMBS Conf.,* San Diego, August, 2012, pp. 5887–5890.

[7] http://www.microsoft.com/en-us/kinectforwindows/.

[8] E. Stone and M. Skubic, "Evaluation of an Inexpensive Depth Camera for Passive In-Home Fall Risk Assessment," in *Proc. Pervasive Health Conference*, Dublin, Ireland, 2011, pp. 71-77.

[9] E. Stone and M. Skubic, "Unobtrusive, Continuous, In-HomeGait Measurement Using the Microsoft Kinect," *IEEE Transactions on Biomedical Engineering*, vol. 60(10), pp. 2925-2932, 2013.

[10] L. G. Shapiro and G. C. Stockman, "Computer Vision," pp. 137, 150, *Prentice Hall*, 2001.

[11] R. O. Duda and P. E. Hart, "Use of the Hough Transformation to Detect Lines and Curves in Pictures," *Comm. ACM*, vol. 15, pp. 11–15.